

Evidence of Piezoelectricity in SWNT-Polyimide and SWNT-PZT-Polyimide Composites

ZOUBEIDA OUNAIES*

Texas A&M University, College Station, TX 77843, USA

CHEOL PARK

National Institute of Aerospace, Hampton, VA 23681, USA

JOYCELYN HARRISON AND PETER LILLEHEI

NASA Langley Research Center, Hampton, VA 23681, USA

ABSTRACT: Nanotechnology offers opportunities to reenergize the area of smart materials by addressing their current shortfalls and expanding their application range. For example, sensors based on polymer nanocomposites would provide a new paradigm for lightweight structural health monitoring for broad aeronautics and space applications. Deployable structures such as inflatable antennae and space mirrors will benefit from the incorporation of multifunctional lenses employing smart, articulating materials. In this paper, an approach to enhance the piezoelectricity of polyimides through the addition of lead zirconate titanate (PZT) particles and single-wall carbon nanotubes (SWNT) is presented. The dielectric and electrical properties of the composites are investigated as a function of SWNT volume content. The dynamic and static mechanical properties are presented to assess the effect of the inclusions on the macro-scale properties of the nanocomposites. It is found that the SWNTs increase the dielectric, piezoelectric, and mechanical properties of the polyimide matrix. Addition of the SWNT in the PZT/polyimide composites facilitates poling and results in an increase of the piezoelectric properties of the three-phase composite.

KEY WORDS: piezoelectric polyimide, single-wall carbon nanotube, lead zirconate titanate, nanocomposite.

*Author to whom correspondence should be addressed. E-mail: zounaies@tamu.edu
Figures 4–9 appear in color online <http://jtc.sagepub.com>

INTRODUCTION

NASA AND OTHER government agencies have fundamental needs for viable materials-based solutions to meet the demands of multifunctional, lightweight skins for morphing and adaptive structures, unmanned aerial vehicles (UAVs), and deployable space structures. Sensors based on polymer nanocomposites would provide a new paradigm for lightweight structural health monitoring for broad aeronautics and space applications. Deployable structures such as inflatable antennae and space mirrors will benefit from the incorporation of multifunctional lenses employing smart, articulating materials. Conventional piezoelectric ceramics such as lead zirconate titanate (PZT) exhibit high electromechanical coupling coefficients ($k \sim 0.4$), a wide range of dielectric constant values (500–4000), and tailorable dielectric and mechanical losses. However, they also exhibit large acoustic and mechanical impedance, resulting in a poor match to soft media such as organic tissue and water [1]. In contrast, piezoelectric semicrystalline polymers have excellent acoustic matching, high flexibility, low dielectric constant values, and high dielectric breakdown. The disadvantages include low electromechanical coupling coefficients and low operating temperatures [2]. Amorphous polymers are an alternate type of piezoelectric polymers. One of the most important properties of an amorphous piezoelectric polymer is its glass transition temperature T_g (temperature below which the material exhibits glass-like characteristics, and above which it has rubber-like properties), which dictates use of temperature and determines the poling process conditions. The piezoelectricity in amorphous polymers differs from that in semicrystalline polymers in that the polarization is not in a state of thermal equilibrium, but rather a quasi-stable state due to the freezing-in of molecular dipoles. Dipolar orientation is induced by applying an electric field, E_p , at an elevated temperature ($T_p \geq T_g$) where the molecular chains are sufficiently mobile to allow dipole orientation with the electric field. Partial retention of this orientation is achieved by lowering the temperature below T_g in the presence of E_p , resulting in a piezoelectric-like effect. The remanent polarization, P_r is directly proportional to E_p and the piezoelectric response, and it is simply the instantaneous polarization during poling minus the electronic and atomic polarizations that relax at room temperature once the field E_p is removed. The following linear equation for P_r results when the Clausius Mossotti equation is used to relate the dielectric constant to the dipole moment [3]:

$$P_r = \Delta \varepsilon \varepsilon_0 E_p \quad (1)$$

where $\Delta\epsilon$ is the dielectric relaxation strength, the difference between the dielectric constant value above and below T_g , and ϵ_0 is the permittivity of free space ($8.85 \times 10^{-12} \text{ F m}^{-1}$). Broadhurst et al. [4] presented a theoretical model for polymers with frozen-in dipolar orientation to explain piezoelectricity and pyroelectricity in amorphous polymers. The dielectric relaxation strength, $\Delta\epsilon$ may be the result of either free or cooperative dipole motion. Equation 1 illustrates that P_r and hence the piezoelectric response is determined by $\Delta\epsilon$, making it a practical criterion to use when designing piezoelectric amorphous polymers.

The literature on piezoelectric amorphous polymers is much more limited than that for semicrystalline polymers. This is due in part to the fact that to date, no piezoelectric amorphous polymers have exhibited responses high enough to attract commercial interest. Much of the previous work on piezoelectric amorphous polymers resides in the area of nitrile substituted polymers including polyacrylonitrile (PAN) [5,6], poly(vinylidene cyanide vinylacetate) (PVDCN/VAc) [7,8], polyphenylethernitrile (PPEN) [9] and poly(1-bicyclobutanecarbonitrile) [10]. In our group, we have developed amorphous polyimides containing polar functional groups [11–13] and investigated their potential use as high temperature piezoelectric sensors. The (β -CN) APB/ODPA polyimide is one such system. The P_r of this piezoelectric polyimide is relatively low, $\sim 14 \text{ mc} \cdot \text{m}^{-2}$ when poled at 100 MV m^{-1} for 1 h above T_g , however, excellent thermal stability was observed up to 100°C , and no loss of the piezoelectric response was seen after aging at 50°C and 100°C up to 500 h [13]. In general, although piezoelectric amorphous polymers have been developed to increase the use temperature of piezoelectric polymers, they too have low piezoelectric coefficients, including a low electromechanical coupling coefficient [2,12]. To overcome these shortcomings, researchers have combined polymers and ceramics, with the hopes of fabricating a strong, flexible composite with tailorable piezoelectric properties [14–17]. Newnham et al. [18] established the concept of connectivity to describe the spatial relationships in a two-phase composite. Composites with 0–3 connectivity are typically composed of a polymer matrix with ceramic particles [19]. They have advantages over other composites in terms of ease of manufacturability and flexibility in controlling particular properties such as mechanical, electrical, and thermal. A main challenge is the poling of such composites. The ratio of resistivity or dielectric constant of the constituent phases is the controlling parameter since it governs the effective poling field across each phase. In 0–3 composites, the effective field can be one or two order of magnitude lower than the applied field [20]. The reason is that most polymers have a lower dielectric constant and higher resistivity than ceramics; therefore, most of the poling field will be concentrated in the lower dielectric phase. One way to

pole the 0–3 composite is to decrease the resistivity of the polymer matrix by the introduction of a conductive third phase such as carbon black. By controlling the volume fraction of the conductive phase, a continuous electric flux between the ceramic particles is established whereby poling can be induced in the composite [21]. Typically, however, carbon black degrades some of the physical properties of the composite. An appreciable conductivity change can only be achieved at high loadings; however, higher loadings of carbon black generally lead to a deterioration of the mechanical properties and render the processing more difficult [22,23]. In this paper, a small volume fraction of single-wall carbon nanotubes (SWNT) is added to raise the dielectric constant and lower the resistivity of the polymer matrix. As a first step, the thermal, dielectric, mechanical, and piezoelectric properties of the resulting SWNT-polyimide composites are studied. This is done in order to select the appropriate SWNT volume content that would lead to improved poling without detrimentally affecting chemical, thermal and mechanical stability of the polymer matrix. The next step is to fabricate the three-phase SWNT–PZT-polyimide composite, and assess the resulting mechanical, dielectric and piezoelectric properties. A piezoelectric aromatic polyimide is used as the matrix to prepare SWNT reinforced polymer composites (Figure 1). The (β -CN) APB/ODPA polyimide possesses the three dipole functionalities shown in Table 1. The nitrile dipole is pendant to a phenyl ring ($\mu = 4.18$ D), while the two anhydride dipoles ($\mu = 2.34$ D) and the diphenylether groups are within the chain, resulting in a total dipole moment per repeat unit of 10.1 D.

Several publications document the challenges encountered and the progress made in dispersing, processing, and characterization of SWNT-polymer composites [24–27]. Difficulty in obtaining homogeneously dispersed SWNT-polymer composites arises from the non-reactive nature of the SWNT surface and the unavoidable bundle formation due to van der Waals attraction during synthesis. In this paper, we adopt a method we previously developed to efficiently disperse SWNT into the polymer matrix on a nanoscale level [28,29].

EXPERIMENTAL

Nanocomposite Processing

Purified SWNTs processed using high pressure carbon monoxide (HiPco) were purchased from CNI (Houston, TX, USA). The diameter of SWNT is in the range of 0.85–1.22 nm based on Raman spectroscopy. The SWNT-polyimide composites were prepared by *in situ* polymerization under sonication. The density of pure polyimide is about 1.3 g cm^{-3} , and

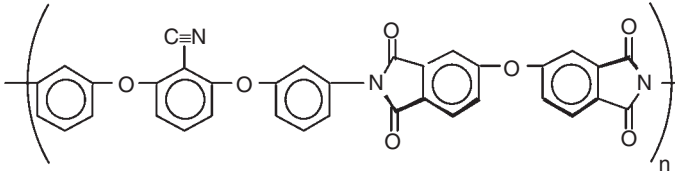

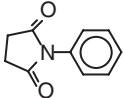
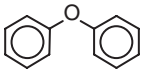


Figure 1. Chemical structure of (β-CN) APB/ODPA.

Table 1. Values of the dipole moments within the nitrile-substituted polyimide.

Dipoles	Dipole identity	Dipole moment (Debye)
	Pendant nitrile group	4.18
	Main chain dianhydride group	2.34
	Main chain diphenylether group	1.30

the calculated density of the SWNT ranges from 1.33 to 1.40 depending on chirality [28]. The diamine and dianhydride used to synthesize the nitrile polyimide were 2,6-bis(3-aminophenoxy) benzonitrile ((β-CN)APB) and 4,4'-oxydipthalic anhydride (ODPA), respectively [30]. To prepare the SWNT-polyimide two-phase composite, SWNT dispersed in anhydrous dimethyl acetamide (DMAc) was used as a solvent for the poly(amic acid) synthesis. The entire reaction was carried out with stirring, in a nitrogen-purged flask immersed in a 40 kHz ultrasonic bath until the solution viscosity increased and stabilized. Sonication was terminated after 3 h and stirring was continued for several hours to form a SWNT-poly(amic acid) solution. The resulting solution was cast onto a glass plate and dried in a dry air-flowing chamber. Subsequently, the dried tack-free film was thermally cured in a nitrogen oven to obtain solvent-free freestanding SWNT-polyimide film. A series of SWNT-polyimide nanocomposite films were prepared with SWNT concentrations ranging from 0.01 to 2.0 vol%. A similar procedure was followed to make the SWNT-PZT-polyimide composites. In addition to dispersing the SWNT in

DMAc prior to the poly(amic acid) synthesis, PZT sub-micrometer powders were also dispersed in SWNT-DMAc suspension.

Thermal and Mechanical Characterization

Glass transition temperatures of the films were determined by differential scanning calorimetry (DSC) using a TA Instruments Q-1000 at a heating rate of $10^{\circ}\text{C min}^{-1}$. Dynamic mechanical measurements were taken on a Rheometrics RSA II instrument in tensile mode at a strain of 0.2% using a temperature sweep from 25°C to 300°C , with a heating rate of $2^{\circ}\text{C min}^{-1}$, at two discrete frequencies of 1 Hz and 10 Hz. The storage modulus, loss modulus, and loss tangent were recorded for every sample tested. Sample dimensions were $\sim 1.25 \text{ in.} \times 0.25 \text{ in.}$ Tensile properties of the composite films were measured by an Instron microtester (Model 5848) according to ASTM D882. High-resolution scanning electron microscopy (HRSEM), Hitachi model S-5200, was used to visualize and qualitatively assess the dispersion in the two-phase and three-phase composites.

Dielectric and Piezoelectric Characterization

Dielectric and piezoelectric properties of the composites were measured. Dynamic dielectric spectroscopy (DDS) provides information about the segmental mobility of a polymer by probing its dielectric properties. The complex dielectric properties, namely the dielectric constant ε' and the dielectric loss ε'' , are determined by performing scans as a function of frequency. The dielectric constant ε is given by

$$\varepsilon = \varepsilon' - i\varepsilon'' \quad (2)$$

After each frequency scan, the temperature is increased to better probe relaxation phenomena. A low AC external electric field ($V_{\text{rms}} = 0.005\text{--}1.0 \text{ V}$) is applied across the material in a (parallel plate) configuration. The observed dielectric relaxation is the result of a movement of dipoles or electric charges due to a changing electric field in the frequency range of interest. An HP4284A Precision LCR meter and a Sun Systems Environmental Chamber are used to perform the dielectric spectroscopy. A Labview program controls both the frequency and the temperature of measurement, records the capacitance and loss tangent, and converts the raw data to dielectric constant and dielectric loss.

Thermally stimulated current (TSC), sometimes referred to as thermally stimulated discharge (TSD) or thermally stimulated depolarization current

(TSDC), is a powerful tool for measuring the release of stored dielectric polarization in the form of charge or current. The charge in a polymer may be generated by various mechanisms, such as orientation of permanent dipoles, trapping of real charges by structural defects or impurities, or ionic or electronic build-up near inhomogeneities and interfaces. While DDS yields the *predicted* piezoelectric performance through the calculation of $\Delta\varepsilon$ (Equation (1)), TSC yields the *actual* piezoelectric performance by measuring P_r [12,13]. A SETARAM TSC 3000, automated TSC equipment, is used to track the relaxation processes in the polymer composites. The apparatus has a temperature range from -180 to 400°C , and a voltage up to 500 V . First, the sample is inserted between two electrodes and a voltage is applied at a temperature T for a fixed time t . Second, the sample is then cooled under electric field. Finally, the sample is reheated at a constant rate ($1\text{--}2^\circ\text{C min}^{-1}$), and the current is monitored. Heating of the sample at a constant rate accelerates the real charge decay, which can be observed as a current release. Current is monitored as a series of peaks, the shape and location of which can be related to dipole orientation (P_r) and charge migration.

RESULTS

SWNT-polyimide and SWNT-PZT-polyimide composites were prepared by *in situ* polymerization in the presence of sonication. No significant change in the glass transition temperature, T_g , of the composites was observed, indicating that the polyimide condensation reaction was not adversely affected by the incorporation of SWNT and sonication. T_g was in the range of $209\text{--}214^\circ\text{C}$ (Table 2).

In the case of SWNT-((β -CN)APB/ODPA), HRSEM micrographs revealed that thin SWNT bundles were dispersed uniformly throughout the whole polymer matrix (Figure 2) as described by two of the co-authors in [31].

Similarly, the SWNT-PZT-(β -CN APB/ODPA) also showed good dispersion of the PZT particles in the SWNT-polyimide matrix (Figure 3). The PZT particles appear to be $<1\ \mu\text{m}$ in diameter with no percolation or connectivity between the PZT particles at this particular volume content.

Table 2. Glass transition temperature values.

Material	T_g ($^\circ\text{C}$)
Polyimide	209.6
Polyimide + 0.2 vol% SWNT	210.0
Polyimide + 1 vol% SWNT	212.8
Polyimide + PZT	213.2

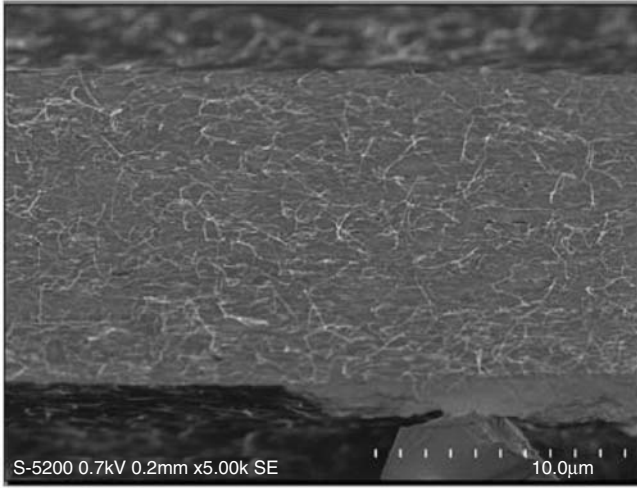


Figure 2. HRSEM of 0.5 vol% SWNT-(β -CN APB/ODPA) [31]. The scale bar is 10 μm .

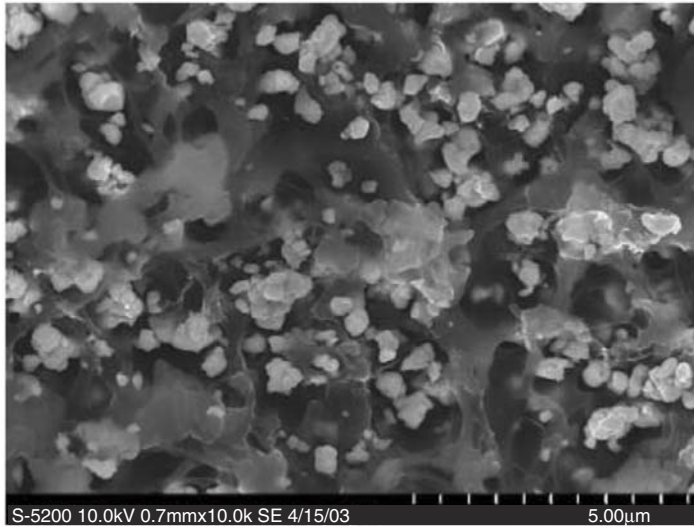


Figure 3. HRSEM of SWNT-PZT-(β -CN APB/ODPA). The PZT-polyimide are 50–50 by weight. The SWNT is 0.1% by weight and volume. The scale bar is 5 μm .

Figure 4 shows the electrical conductivity, σ , as a function of SWNT content. A sharp increase in the electrical conductivity was observed between 0.02 and 0.1 vol%, where σ changed from 4×10^{-14} to 10^{-7}Scm^{-1} . This increase continues to 1 vol% SWNT where the value reaches 10^{-4}Scm^{-1} .

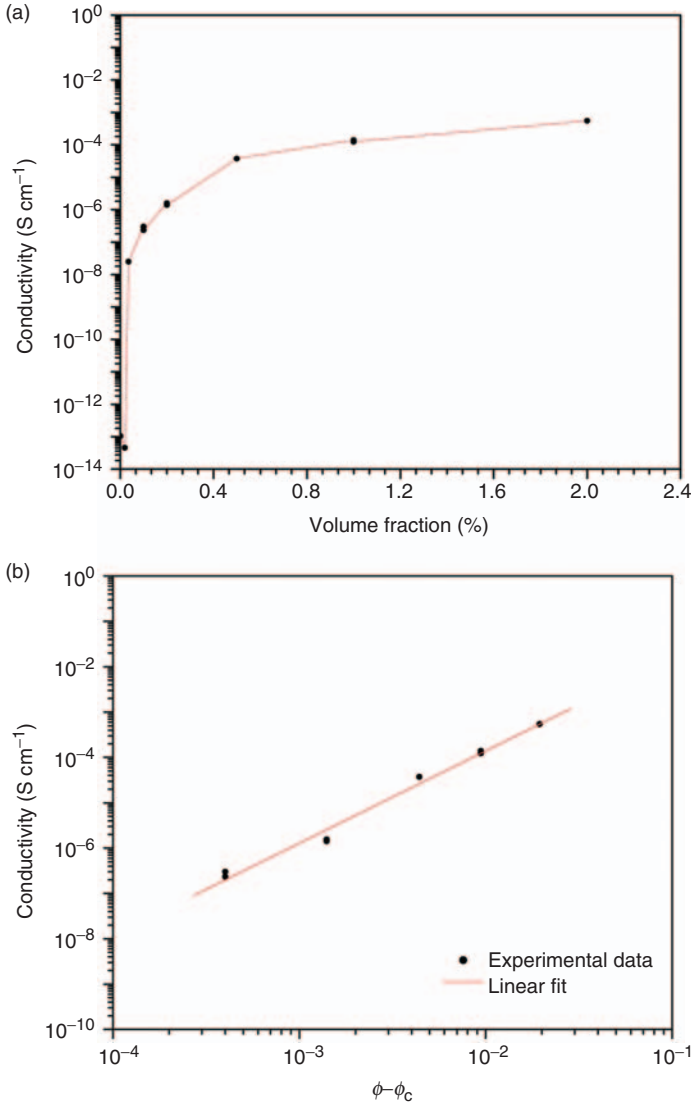


Figure 4. (a) Electrical conductivity as a function of SWNT volume fraction ($f=20\text{ Hz}$); (b) Percolation behavior of SWNT-polyimide composites.

This behavior is indicative of a percolation transition. Percolation theory [32,33] predicts that there is a critical concentration or percolation threshold at which a conductive path is formed by the inclusions in the composite, causing the material to convert from an insulator to a conductor.

Figure 4(a) indicates that the percolation threshold for this material resides between 0.02 and 0.1 vol%. In order to better determine the critical volume concentration, the experimental data was fitted using the classical percolation power law [32–34]. The electrical conductivity was found to obey the relationship described by Equations 3(a) and 3(b):

$$\sigma = A(\phi - \phi_c)^t \quad (3a)$$

$$\log \sigma = \log A + t \log(\phi - \phi_c) \quad (3b)$$

where σ is the electrical conductivity of the composite, ϕ is the volume fraction of the SWNT in the composite, ϕ_c is the critical volume fraction (volume fraction at percolation), A and t are fitted constants. Using Equation 3(b), Figure 4(b) shows a good fit was achieved between the experimental data (solid circles) and the fit function (straight line), with a correlation factor $R = 99.9\%$. A best fit to the data identifies ϕ_c at 0.06 vol% (percolation threshold value). The low value of the percolation threshold is indicative of good dispersion. Next, the effect of SWNT addition on dipolar orientation in the polyimide films is investigated by DDS as function of temperature, in the vicinity of percolation (0–0.1 vol%). These measurements yield the dielectric relaxation strength $\Delta\epsilon$ discussed in a previous section, where the larger the value of $\Delta\epsilon$, the higher the piezoelectric performance (Equation (1)). Figure 5 shows the dielectric constant as a function of temperature at 1 kHz.

The dielectric constant does not vary much with temperature below T_g ($\sim 210^\circ\text{C}$). As the temperature approaches T_g however, the dielectric constant increases because dipolar relaxation within the polyimide starts contributing to its value [2,3]. The resulting $\Delta\epsilon$ value is ~ 6 at 1 kHz for the unfilled polyimide. Adding increasing amounts of SWNT not only raises the value of the dielectric constant but also increases the value of $\Delta\epsilon$. At 0.1 vol%, the value of the dielectric constant increases almost four-fold, from 3.5 to 11. For that same composition, $\Delta\epsilon$ improves from 6 to 20. The increase in $\Delta\epsilon$ indicates that the presence of the SWNT enhances orientation polarization, and therefore, may lead to a higher piezoelectric performance. Poling of the SWNT-polyimide composites confirms this observation. As shown in Table 3, three different concentrations were poled at 50 MV m^{-1} : the pristine polyimide, the 0.02 vol% SWNT + polyimide, and the 0.1 vol% SWNT + polyimide. After poling the composites, the remanent polarization, P_r , was measured using the TSC method. P_r increases with increasing content of SWNT even though the poling conditions remain the same for all three cases. As predicted by the measurement in Figure 5, at 0.1 vol%, P_r is 32, more than four times the value for the pristine polyimide.

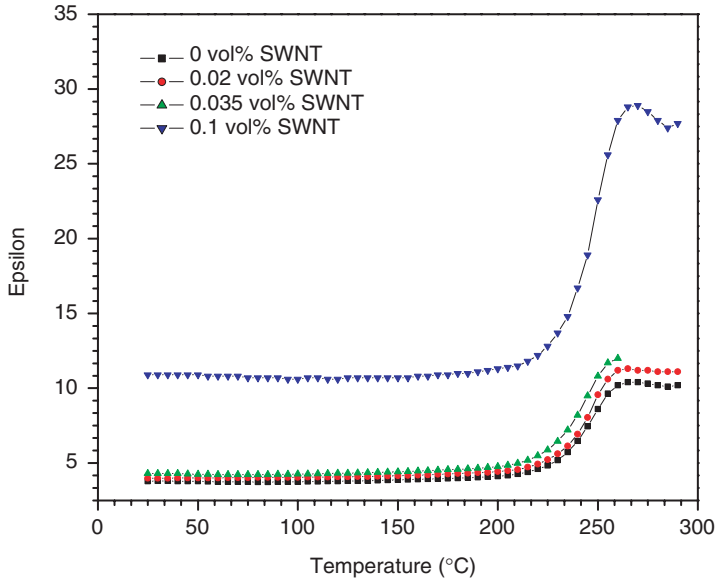


Figure 5. Dielectric relaxation strength as a function of temperature for SWNT-polyimide composites. ($f = 1 \text{ kHz}$)

Table 3. Remanent polarization comparison for the 2-phase composite.

Material	$E_p \text{ (MV m}^{-1}\text{)}$	$P_r \text{ (mC m}^{-2}\text{)}$
Piezoelectric polyimide	50	7
0.02 vol% SWNT-polyimide	50	15
0.1 vol% SWNT-polyimide	50	32

The presence of the SWNT leads to better dipolar alignment with the poling field, and possibly indicate that a higher number of dipoles have realigned in the direction of the electric field.

In Figure 6, three cases are shown: the pristine polyimide (0 vol% SWNT), the 0.1 vol% SWNT + polyimide, and the 0.1 vol% SWNT + 20 vol% PZT + polyimide. The value of $\Delta\epsilon$ for the three-phase composite, 0.1 vol% SWNT + 20 vol% PZT + polyimide, is 90. It is noted that when 20 vol% PZT was added to the polyimide without SWNT, the dielectric constant of the composite did not vary significantly from that of the polyimide (increased from 4 to 6), and no measurable increase in $\Delta\epsilon$ was observed. This result confirms that PZT cannot be poled in the polyimide/PZT composite without the help of the SWNT as third phase. The presence of SWNT decreases the mismatch between the dielectric constant of the polyimide and that of the PZT.

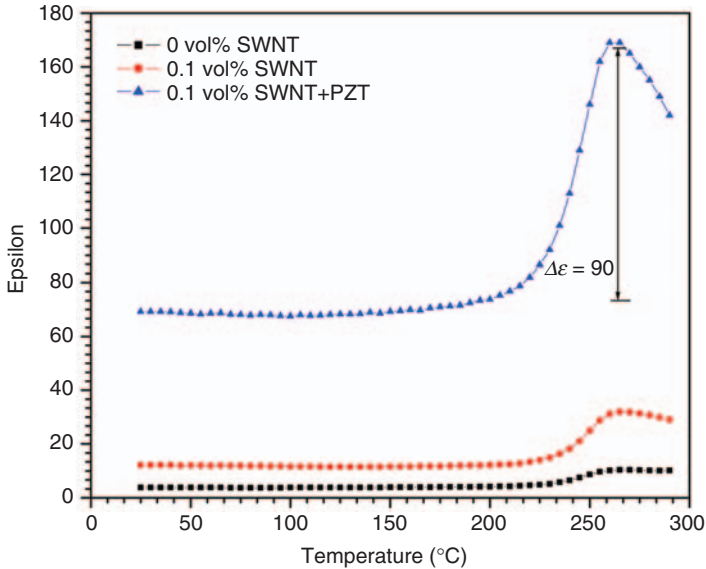


Figure 6. Dielectric constant as a function of temperature for the two-phase and three-phase composites.

Table 4. Remanent polarization comparison for the 3-phase composite.

Material	E_p (MV m^{-1})	P_r (mC m^{-2})
Piezoelectric polyimide	50	7
PZT-polyimide	50	11
0.1vol%SWNT–PZT-polyimide	50	84

Table 4 presents the results of poling the three-phase composite. The remanent polarization values were measured using TSC after poling. As predicted by Figure 6, the three-phase composite displays a dramatic increase in P_r , from 7 to 84. This increase confirms that the presence of SWNT raised the dielectric constant of the composite matrix such as it was possible to pole the PZT particles and the polyimide simultaneously.

The mechanical properties of the two-phase and three-phase composites were measured by DMA to assess the effect of adding the SWNT and PZT inclusions on the modulus of the polyimide.

DMA results (Figure 7) reveal that some reinforcement occurs at temperatures below T_g due to the addition of SWNT, where up to 50% increase is measured at 50°C. A larger reinforcement is seen at temperatures higher than T_g (Figure 7). Above T_g , the 2.0 vol% SWNT have a stronger effect than the 0.1 vol% SWNT on the modulus of the polyimide. Figure 8

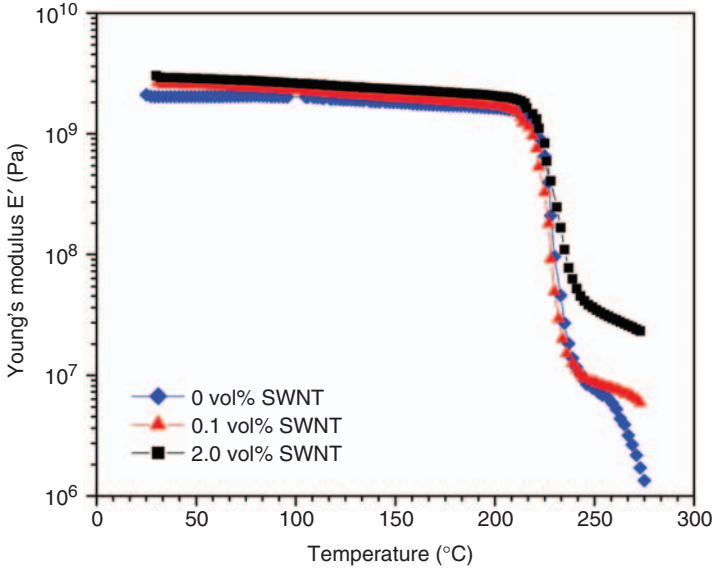


Figure 7. Young's modulus (storage modulus), E' of the polyimide and SWNT-polyimide composites at 1 Hz.

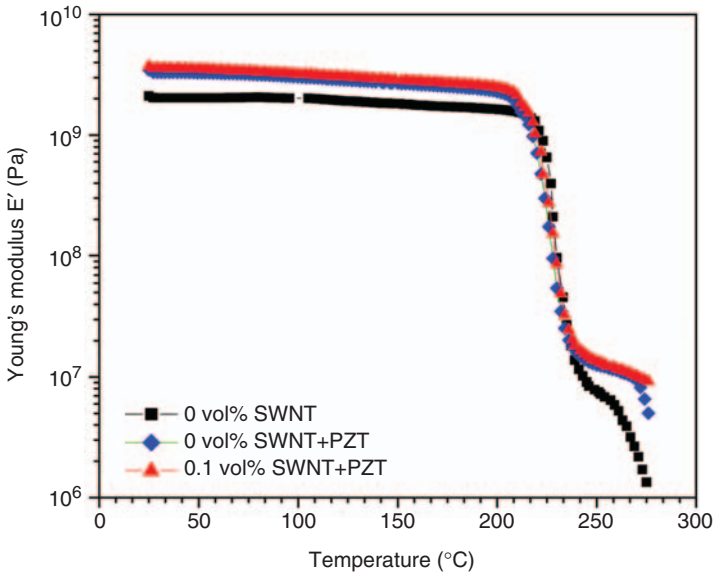


Figure 8. Young's modulus (storage modulus), E' , of the polyimide, PZT-polyimide and SWNT-PZT-polyimide composites at 1 Hz.

shows the effect of adding PZT on the modulus of the polyimide. Again, more reinforcement is obtained at temperatures higher than T_g than at ones lower than T_g . However, the reinforcement is higher both below and above T_g , probably owing to the high volume content of the PZT as compared to the SWNT. Additionally, the $\tan \delta$ peak, corresponding to T_g , shifts to slightly higher temperature with increasing inclusion content in the nanocomposites (Figure 9 compares 0.0 vol% and 2.0 vol% SWNT) compared to the pristine polymers; these peaks also decrease in intensity. This observation indicates weakened cooperative relaxation of the polymer chains in the composite due to the restriction of chain mobility at the inclusions. The static tensile test results (Table 5) are consistent with the DMA results, and show moderate increase of modulus below T_g . At 2.0 vol% SWNT loading, both modulus and strength increased with the

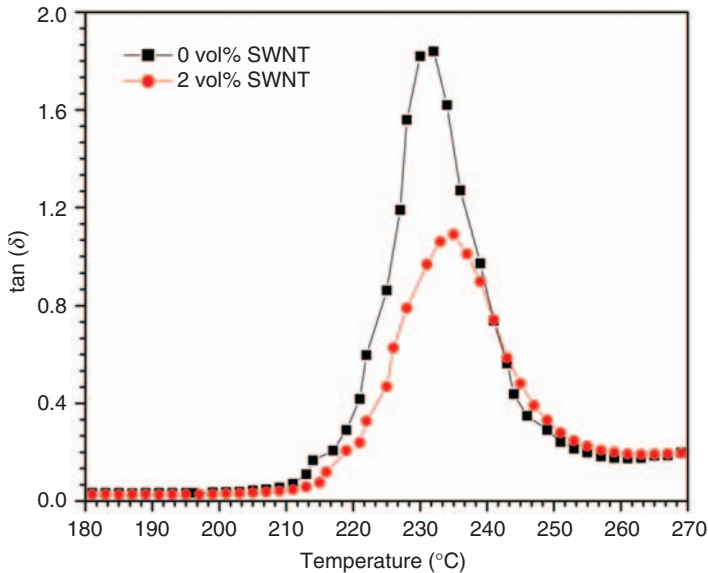


Figure 9. Comparison of $\tan \delta$ for two SWNT-polyimide compositions.

Table 5. Tensile measurements.

	Tensile modulus (GPa)	Tensile strength (MPa)	Break elongation (%)
(β -CN)APB/ODPA	2.74 ± 0.8	133 ± 4	7.7
2 vol% SWNT	3.36 ± 2.8	139 ± 2	7.8
5 vol% SWNT	3.96 ± 0.7	123 ± 6	7.0

same elongation at break. At 5.0 vol% SWNT, the modulus increased by 44%. The sample dimensions were 5×50 mm (width \times gage length) and the thickness was ~ 50 – 80 μm .

CONCLUSION

An approach to enhance the piezoelectricity of polyimides through the addition of PZT and SWNT is presented. Specifically, this paper addresses one of the challenges in poling a 0–3 composite by adding a low volume content of a third conducting phase, namely SWNTs. Thermal characterization through DSC confirms that the presence of SWNTs do not detrimentally affect the physical properties of the polyimide matrix. Improvement in the mechanical properties of the SWNT-PZT-polyimide composites resulted from the dual presence of SWNT and PZT, as was demonstrated by DMA measurements. $\tan \delta$ measurements indicate a possible decrease in polymer chain mobility in the presence of higher content SWNT (>2 vol%). Additional measurements at higher volume content SWNTs are being conducted to confirm this behavior. Next, dielectric spectroscopy as a function of SWNT content shows a low percolation threshold of 0.06 vol%, indicating a uniform dispersion of the nanoinclusions in the polyimide. DDS measurements as a function of temperature reveal a relaxation behavior in the SWNT-polyimide composites, quantified by the dielectric relaxation strength $\Delta\epsilon$. The dielectric relaxation occurs at T_g , which indicates that it is inherent to the polyimide. The increase observed in $\Delta\epsilon$ puts in evidence a strong interaction between the SWNT and the polyimide dipoles. Both the presence of a large interfacial polarization due to SWNTs and/or SWNTs essentially extending the electrodes into the polymer matrix and raising the local field values are thought to induce the high dielectric constant values and the measured increase in P_r . The nature of this interaction, and the polarization and local field mechanisms are currently under investigation. Addition of the SWNT in the PZT/polyimide composites facilitates poling of the polyimide, and yields a higher P_r values at the same poling conditions. At 0.1 vol% SWNT, the value of P_r is one order of magnitude higher than that of the pristine polyimide. Increase in the piezoelectric coefficients is expected to mirror that of P_r . It is important to note that the increase in P_r was achieved at a relatively low loading of PZT particles (20 vol%). Because the PZT particles did not achieve percolation, the composite remained flexible and was relatively easy to process. As a result, a standard polymer casting technique was utilized to prepare the three-phase composite.

ACKNOWLEDGMENTS

The authors acknowledge David Callahan for writing Labview programs to facilitate data gathering. Z.O. research is supported in part by NASA Grant no. NCC1-02013. Z.O. appreciate support from the NASA University Research, Engineering and Technology Institute on Bio Inspired Materials (BIMat) under award no. NCC-1-02037. Finally, the authors wish to thank Dr. Ricardo Perez for his helpful comments on the manuscript.

REFERENCES

1. Jaffe, B., Cook Jr, W.R. and Jaffe, H. (1971). *Piezoelectric Ceramics*, Academic Press, London, New York.
2. Davis, G.T. (1993). Piezoelectric and Pyroelectric Polymers. *Polymers for Electronic and Photonic Applications*, p. 435, Academic Press, Boston, MA, USA.
3. Hilczer, B. and Malecki, J. (1986). *Electrets: Studies in Electrical and Electronic Engineering* 14, p. 19, Elsevier, New York, NY.
4. Broadhurst, M.G., Malmberg, C.G., Mopsik, F.I. and Harris, W.P. (1973). Piezo- and Pyroelectricity in Polymer Electrets, In: Perlman, M.M. (ed.), *Electrets: Charge Storage and Transport in Dielectrics*, pp. 492–504, The Electrochemical Society, Princeton, NJ.
5. Ueda, H. and Carr, S.H. (1984). Piezoelectricity in Polyacrylonitrile, *Poly. J.*, **16**: 661–667.
6. von Berlepsch, H., Kunstler, W., Wedel, A., Danz, R. and Geib, D. (1989). Piezoelectric Activity in a Copolymer of Acrylonitrile and Methylacrylate, *IEEE Trans. Elec. Ins.*, **24**: 357–362.
7. Seo, I. (1995). Piezoelectricity of Vinylidene Cyanide Copolymers and Their Applications, *Ferroelectrics*, **171**: 45–55.
8. Mirau, P.A. and Heffner, S.A. (1992). Chain Conformation in Poly(vinylidene cyanide-vinyl acetate): Solid State and Solution 2D and 3D n.m.r. Studies, *Polymer*, **33**: 1156–1161.
9. Tasaka, S., Toyama, T. and Inagaki, N. (1994). Ferro- and Pyroelectricity in Amorphous Polyphenylethnitrile, *Jpn J. Appl. Phys.*, **33**: 5838–5844.
10. Hall, H.K., Chan, R.J.H., Oku, J., Hughes, O.R., Scheinbeim, J. and Newman, B. (1987). Piezoelectric Activity in Films of Poly(1-bicyclobutanecarbonitrile), *Poly. Bull.*, **17**: 135–136.
11. Ounaies, Z., Park, C., Harrison, J.S., Smith, J.G. and Hinkley, J. (1999). Structure-Property Study of Piezoelectricity in Polyimides, In: *SPIE Proceedings, Electroactive Polymer Actuators and Devices*, In: Yoseph Bar-Cohen (ed.), Vol. 3669, p.171, Newport Beach, CA.
12. Harrison, J. and Ounaies, Z. (2002). *Encyclopedia of Smart Materials*, In: Biderman, A. (ed.), John Wiley and Sons, New York, 162–173.
13. Park, C., Ounaies, Z., Wise, K. and Harrison, J. (2004). In Situ Poling and Imidization of Amorphous Piezoelectric Polyimides, *Polymer*, **45**(16): 5417–5425.
14. Dias, C.J. and Das-Gupta, D.K. (1996). *IEEE Trans. Dielect. Elec. Ins.*, **3**: 706.
15. Safari, Y., Lee, H., Halliyal, A. and Newnham, R.E. (1987). *Amer. Ceram. Soc. Bull.*, **66**: 668.
16. Hanner, K.A., Safari, A., Newnham, R.E. and Runt, J. (1989). *Ferroelectrics*, **100**: 255.
17. Lushcheikin, G.A., Astafyev, A.V. and Lazareva, N.A. (1989). *Ferroelectrics*, **94**: 453.
18. Newnham, R.E., Skinner, D.P. and Cross, L.E. (1978). *Mat. Res. Bull.*, **13**: 525–536.
19. Sakamoto, W.K., de Souza, E. and Das-Gupta, D.K. (2001). *Mat. Res.*, **4**: 201–204.

20. Furukawa, T., Ishida, K. and Fukada, E. (1979). *J. Appl. Phys.*, **50**: 4904.
21. Sa-Gong, G., Safari, A., Jang, S.J. and Newnham, R.E. (1986). *Ferroelectr. Lett. Sect.*, **5**: 131–142.
22. Moulart, C. Marrett, and Colton, J. (2004). *Poly. Eng. Sci.*, **44**: 588–597.
23. Saad, L., Aziz, H.A. and Dimitry, O.I.H. (2004). *J. Appl. Poly. Sci.*, **91**: 1590–1598.
24. Shaffer, M. and Windle, A. (1999). *Adv. Mater.*, **11**: 937–941.
25. Sandler, J., Shaffer, M., Prasse, T., Bauhofer, W., Schulte, K. and Windle, A. (1999). *Polymer*, **40**: 5967–5971.
26. Kymakis, E., Alexandou, I. and Amaratunga, G. (2002). *Syn. Met.*, **127**: 59–62.
27. Benoit, J., Benoit, C., Lefrant, S., Bernier, P. and Chauvet, O. (2002). *Mat. Es. Soc. Symp. Proc.*, **706**: Z3.28.1–Z3.28.6.
28. Park, Z., Ounaies, A.K., Watson, R.E., Crooks, J.G., Smith Jr, S., Lowther, J., Connell, E., Siochi, J., Harrison, S. and St.Clair, T.L. (2002). *Chem. Phys. Lett.*, **364**(3–4): 303–308.
29. Ounaies, Z., Park, C., Wise, K., Siochi, E. and Harrison, J. (2003). *Comp. Sci. Tech.*, **63**: 1637.
30. Simpson, J.O., Ounaies, Z. and Fay, C. (1997). Polarization and Piezoelectric Properties of a Nitrik-substituted Polyimide, *Materials Research Society Proceedings: Materials for Smart Systems II*, In: George, E.P., Gotthardt, R., Otsuka, K., Trolrier-McKinstry, S. and Wun-Fogle, M. (eds), Vol. 459, p. 53, Materials Research Society, Pittsburgh, PA.
31. Mclachlon, D.S., Chiteme, C., Park, C., Wise, K.E., Louthier, S.E., Lillehei, P.T., Siochi, E.J. and Harrison, J. (2005). *J. Polym. Sci.: Part B. Phys.*, **43**: 3273–3287.
32. Bergman, J. and Imry, Y. (1977). *Phys. Rev. Lett.*, **39**: 1222–1225.
33. Stauffer, (1991). *Introduction to the Percolation Theory*, Francis and Taylor, London, UK.
34. Potschke, P., Dudkin, S.M. and Alig, I. (2003). *Polymer*, **44**: 5023–5030.